DOI: 10.48011/sbse.v1i1.2301

Use of the Particle Swarm Technique to Optimize Parameters of Photovoltaic Generators on Networks with High Integration of Distributed Generation ⋆

Luiz G. R. Tonini * **Felipe Z. da Silva** * **Renato S. F. Ferraz** *
Oureste E. Batista * **Augusto C. Rueda-Medina** *

* *Federal University of Espírito Santo, ES, luiz.tonini@aluno.ufes.br, felipe.z.silva@aluno.ufes.br, renato.s.ferraz@aluno.ufes.br, oureste.batista@ufes.br, augusto.rueda@ufes.br.*

Abstract: In search of greater diversity in energy sources, to meet the demand of the electricity power, the use of photovoltaic generators is increasing. Such components have their power generation specified by IEEE 1547/2018, which limits the power parameters of each one. In a situation of high penetration of distributed generation, generators can contribute to the electric current that will circulate within the system in case of a fault, causing major disruption to the mesh and the users. Seeking to reduce this impact, the paper will minimize the value of the short circuit current by adjusting the parameters of the photovoltaic generators. The analysis will be done on IEEE Test Feeder 13 and 34 nodes and will refer to generators from category A, B and without reactive power injection in the mesh.

Resumo: Em busca de maior diversidade nas fontes de energia, para suprir a demanda da rede elétrica de distribuição, é cada vez mais comum o uso de geradores fotovoltaicos. Tais componentes têm sua geração de potência especificada pela norma IEEE 1547/2018, que limita os parâmetros de potência de cada nó. Em uma situação de alta penetração de geração distribuída, os geradores podem contribuir com a corrente elétrica que circulará dentro da malha em caso de falta, causando maiores transtornos a rede e aos usuários. Buscando diminuir este impacto o trabalho irá minimizar o valor da corrente de curto circuito por meio do ajuste dos parâmetros dos geradores fotovoltaicos. A análise será feita nas redes de 13 e 34 nós do IEEE e usará como referência geradores das categorias A, B e sem capacidade de injetar reativo na rede.

Keywords: Distributed Generation; Photovoltaic Generators; Particle Swarm Optimization; Short circuit.

Palavras-chaves: Geração Distribuída, Geradores Fotovoltáicos, Otimização por Enxame de Partículas; Curto circuito.

1. INTRODUCTION

Seeking to meet the growing demand for sustainable energy, there is the installation of generators near the consumption centers, which has been called Distributed Generation (DG) (Mendes et al., 2018).

Among the DGs stands out the Photovoltaic (PVDG), composed by a solar panel with a frequency inverter. The inverter is the component responsible for shaping the electrical signal to meet the user's demand, whose parameters are subject in the standart 1547/2018 from Institute of Electrical and Electronics Engineers (IEEE) (IEEE, 2018). This standard states that, for category A and B generators respectively, reactive power may range from -0.25 to 0.44 and -0.44 to 0.44 pu; while active power may range from 0.05 to 1 pu (Vargas et al., 2018).

The choice of these parameters is based on maintaining power quality. Another relevant point to choose from is the impact on fault situations. In this scenario, a power supply from the DG to the short circuit node may occur, aggravating the impact of the fault. This situation can be mitigated by a choice of parameters that consider fault values given the characteristics of the network. With this premise, this paper uses an Optimization technique, Particle Swarm Optimization (PSO) (Kennedy and Eberhart, 1995), to define DG Power Parameters (PP) so that single and three-phase faults have their modules minimized.

2. OPTIMIZATION PROCESS

The Optimization operation is a tool with high resolution speed and adaptation to the model. The optimization problem is compoused by an Objective Function (OF), which defines the equation that will be maximized or minimized, a set of constraints, which are the conditions that the OF must meet to solve the problem (Rueda-Medina

⋆ This study was funded in part by the Coordenadoria de Aperfeiçoamento de Pessoal de Nível Superior - Brazil (CAPES) - Finance Code 001.

and Padilha-Feltrin, 2011). The MathWorks Matlab platform was used to implement the methodology described in the following subsection. The implemented solution technique uses PSO, where a maximum population of fifty species has been defined, with a maximum of ten iterations for reproduction and a penalty of 10^{12}, this methodology was used in similar works to perform the PF (Cui-Ru Wang et al., 2005) and SC (Baghaee et al., 2011) calculation ,just like these parameters (Ferraz et al., 2019).

2.1 Model

In the problem proposed in this work, the OF will be the minimization of the sum of the single-phase, considering all phases, and three-phase fault currents. The choice of this type of short circuit was defined to be, respectively, the most common and the most impactful (Vargas et al., 2018). The OF equation is present in (1).

$$Min \;\; \dot{I}_T = \sum_{i}^{N} \dot{I}_{sini} + \sum_{i}^{N} \dot{I}_{thri} \tag{1}$$

In this equation, where I_T is the total current, I_{sin} and I_{thr} are respectively the single-phase and three-phase fault currents in the node i in a network with N nodes. The current will be obtained in the Short Circuit (SC) calculation, by the Composite Matrix Method (Kersting and Shirek, 2012), shown in (2)-(6):

$$F_{sin_a} : C_{14}, C_{23}, C_{32}, C_{47} = 1 \tag{2}$$

$$F_{sin_b} : C_{21}, C_{33}, C_{15}, C_{47} = 1 \tag{3}$$

$$F_{sin_c} : C_{14}, C_{41}, C_{42}, C_{43}, C_{25}, C_{36} = 1 \tag{4}$$

$$F_{thr} : C_{21}, C_{32}, C_{16}, C_{47} = 1 \tag{5}$$

$$\begin{bmatrix} \dot{I}p_a \\ \dot{I}p_b \\ \dot{I}p_c \\ 0 \\ 0 \\ 0 \\ 0 \end{bmatrix} = \begin{bmatrix} 1 & 0 & 0 & Y_{11} & Y_{12} & Y_{13} & Y_{s_1} \\ 0 & 1 & 0 & Y_{21} & Y_{22} & Y_{23} & Y_{s_2} \\ 0 & 0 & 1 & Y_{31} & Y_{32} & Y_{33} & Y_{s_3} \\ C_{11} & C_{12} & C_{13} & C_{14} & C_{15} & C_{16} & C_{47} \\ C_{21} & C_{22} & C_{23} & C_{24} & C_{25} & C_{26} & C_{47} \\ C_{31} & C_{32} & C_{33} & C_{34} & C_{35} & C_{36} & C_{47} \\ C_{41} & C_{42} & C_{43} & C_{44} & C_{45} & C_{46} & C_{47} \end{bmatrix} \cdot \begin{bmatrix} \dot{I}_a \\ \dot{I}_b \\ \dot{I}_c \\ \dot{V}_a \\ \dot{V}_b \\ \dot{V}_c \\ \dot{V}_g \end{bmatrix} \tag{6}$$

In the matrix present in (6), where C variables can be 1 or zero, depending on the type and location of the fault, Y represents the admittance, obtained by the inverse of the impedance measured to the fault point, which is a input parameter, while V is the pre-fault voltage, which will be obtained by the Power Flow (PF) using Backward Forward/Sweep method (Chang et al., 2007), modified for situations with high DG penetration (Tonini et al., 2019).

In this numerical method, where k is any iteration, the voltage is obtained by the product between the admittance of the branches connected to the reference node by the current contribution to it. In (7), M_z is the impedance matrix of the lines connected to node i, while J_m is the current in the lines, obtained by summing the currents from the end nodes to the starting bus. In (8), used to calculate the current of each node, it is possible to observe the active and reactive power, P_i and Q_i, as well as the parameters x_i and y_i. These variables will be the DG PP of each i node, and the output data from the optimization process.

$$\dot{V}_i^k = \dot{V}_{m_i} - M_Z \cdot \dot{J}_{j_i}^k \therefore \dot{J}_{j_i}^k = -\dot{I}_i^k + \sum_{i}^{N} \dot{J}_{m_i}^k \tag{7}$$

$$\dot{I}_i^k = \left[\frac{P_i \cdot (1 - x_i) + j \cdot Q \cdot (1 - y_i)}{\dot{V}_i^{k-1}} \right]^* - M_{Y_i} \cdot \dot{V}^{k-1} \tag{8}$$

The constraints of the Optimization process will be based on the *Procedimentos de Distribuição de Energia Elétrica no Sistema Elétrico Nacional*(PRODIST) from the *Agência Nacional de Energia Elétrica* (ANEEL) (d. S. Barbosa and Carvalho, 2017), which regulates the voltage limits on the generating node, (8). The IEEE Standard 1545/2018 establishes the active power limits, (9). For the reactive, depend on category, which can be A or B according to (11) or (12), respectively, as shown in Figure 1.

As the reactive injection in the network is an unconsolidated situation, regarding the protection requirement in the distribution mesh, a restriction will be proposed to analyze the impact on PP when a DG is unable to perform this operation, according to (13).

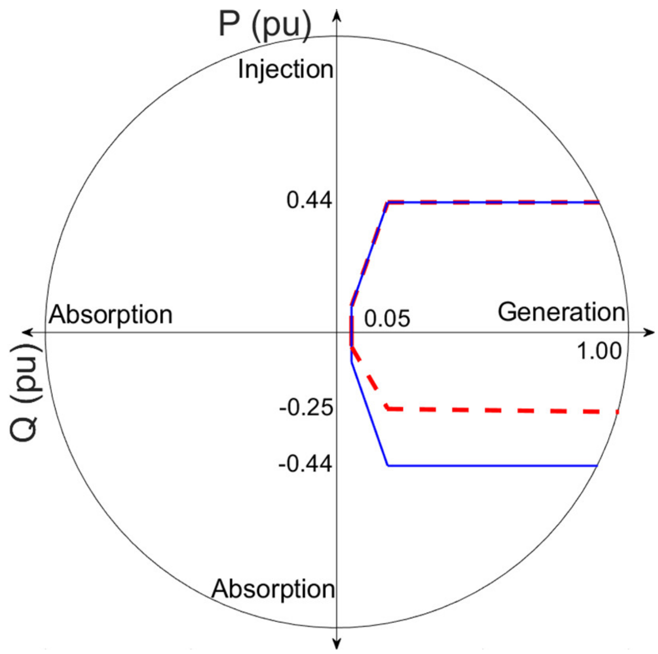

Figure 1. DG, category A and B, maximum and minimum power rating.

$$0.95 \leq V_i \leq 1.05 \tag{9}$$

$$0.05 \leq x_i \leq 1.00 \tag{10}$$

$$-0.25 \leq y'_{Bi} \leq 0.44 \tag{11}$$

$$-0.44 \leq y'_{Ai} \leq 0.44 \tag{12}$$

$$0.00 \leq y''_{i} \leq 0.44 \tag{13}$$

2.2 System

The process begins with the allocation of input parameters: line impedance and admittance, load power and reference bar voltage, with the variables, which are the PP. Is generate an initial population with several variable values, which are subject to restrictions. If the specimens are suitable, reproduction occurs and with them the PF and SC are calculated. Finally, it is verified if the obtained fault current values are local minimums. Having a positive response, the iteration ends, otherwise there is a new selection of variables values until converging to a group of optimized values, or reaching the limit of iterations. The procedure described above, as well as the application of the model, are present in the flowchart of Figure 2.

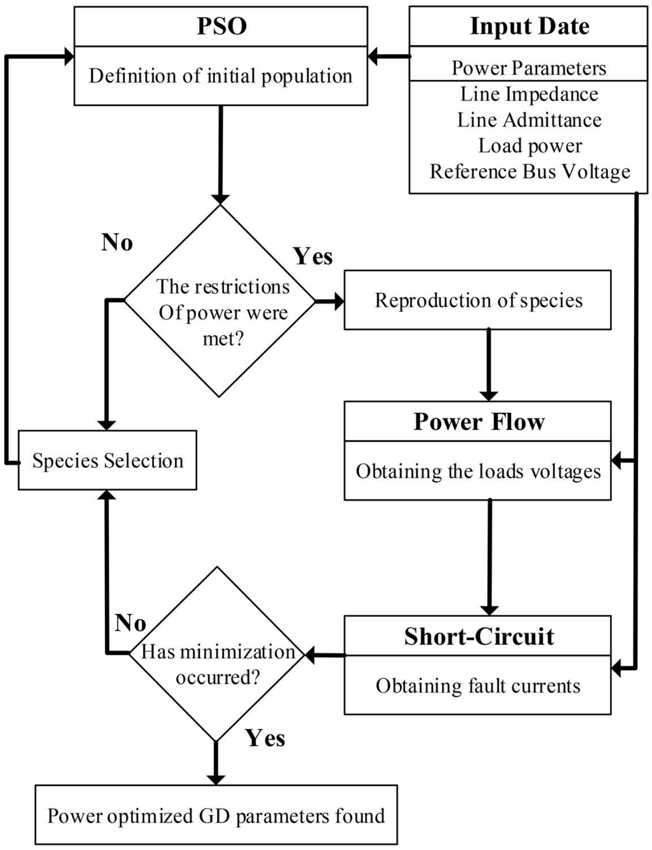

Figure 2. Optimization process flowchart.

3. RESULTS AND DISCUSSION

Aiming to use academically recognized electrical distribution systems with different types of loads, the IEEE Test Feeder of 13 and 34 nodes (Jangra and Vadhera, 2017) were chosen to apply the methodology proposed in this work. Unbalanced loads are present in these systems, which can be one, two or three-phase. As the study focuses on the analysis of short circuit current, the switch between nodes 671 and 692, in the 13 nodes test feeder, will remain closed, while the regulators voltage will be omitted from the calculation.

Applying the methodology of section 2 in the test feeders, where there will be a single phase DG in each phase of each node, which corresponds to a scenario of high penetration of DG, the data present in the appendix Table A.1, and A.2, were obtained. The analysis between the PP from category A with B is present in the subsection 3.1 and between the situation with no reactive power injection, which will be called category Zero, and B in the subsection 3.2. The smallest value of the objective function, for both 13 and 34 nodes, occurs with the parameters in category B, which is $8.334 \cdot 10^{14}$ and $2.811 \cdot 10^{21}$ A, followed very closely by A, with difference only in the nth decimal number, and finally to Zero, that is $8.387 \cdot 10^{14}$ and $2.834 \cdot 10^{21}$ A.

3.1 Categories A and B

From the results of Table A.1, and A.2, it is possible to state that the optimized PP values to minimize the single and three phase fault current in the 13 nodes test feeder are, in most cases, the constraints related to the active and reactive power. This situation is predominant in the 13 nodes test feeder. For the 34 nodes the optimized points varied mostly as in the 13 nodes, but an intermediate PP value, of 0.50 for active power and zero and 0.25 for reactive, appear, as shown in Table A.1, and A.2.

For three-phase loads occurs a situation where one phase operates at maximum limits and the others at minimum. The other analyzes will focus on the PP values and their relation to the quantity, power and locality of the loads.

Load number In the 13 nodes system, the variation of PP values between categories A and B occurred more often than in 34 nodes. This occurrence, for the system with the most nodes, concentrates mainly on the reactive power, while on the least nodes system it is more evenly distributed between active and reactive; and happens mostly on lines 632-634 and 848-860-890, highlighted in blue. This scenario occurs because these loads are one of the farthest from the reference bus and since the short circuit current is inversely proportional to the impedance to the fault point, the contribution of these currents is not as significant as that of the nearest loads. However, as there is a transformer the situation reverses. Thus, to decrease the pre-fault voltage, which depends on PP, due to this component, the parameter changes to inject the maximum reactive power.

Load power The highest system loads are nodes 671, 675, 890 and 844, but only in the 13 nodes system was there variation in these nodes, highlighted in red. In the larger system the PP values tended to the minimum and maximum values in the same proportions for both category A and B.

Location The region with the highest number of phases per node, where PP variation occurred between categories A and B, was in the 34 nodes system, in lines 860-838, highlighted in green. In this region the reactive power parameters were the points of difference. This scenario happened because these loads are the farthest from the reference bus and thus have the highest fault point impedance. And to prevent the pre-fault voltage from reaching values below 0.95 it is necessary to have maximum reactive power, hence the existence in category A of PP equal to zero.

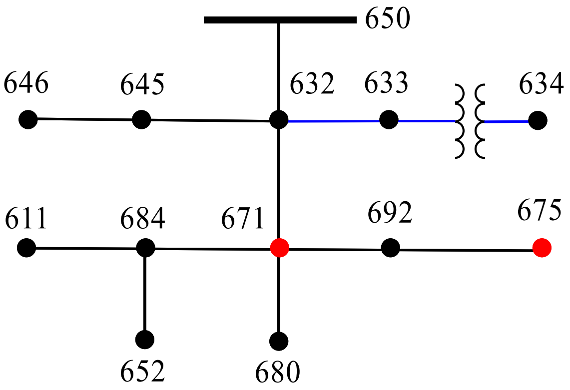

Figure 3. IEEE Test Feeder 13 nodes, category A and B.

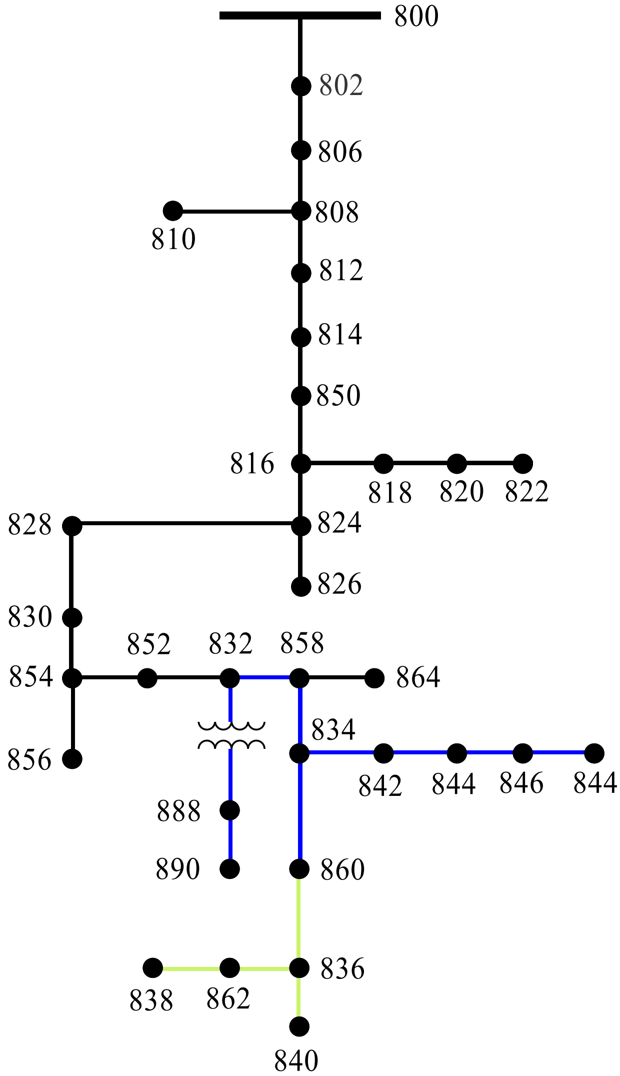

Figure 4. IEEE Test Feeder 34 nodes, category A and B.

3.2 Category Zero and B

With the results of Table A.1, and A.2, it could be assumed that the same PP limit values are found, but not necessarily at the same points. With an intermediate PP value of 0.50 for active power and zero for reactive appear in the 34 nodes. The previous analysis around number, power and location comparing with category B will be done with reference to category zero.

Load number As the number of nodes increases, different values of the limits appear, since at 34 nodes an intermediate value of 0.50 pu for active and zero for reactive arose. This is because the higher the number of nodes, the higher the value of the fault current, so to decrease it is necessary to lower the voltage without extrapolating the limit of 0.95 pu. As a result the apparent power, which having to maintain the power supply, reduces the active power injected by the DG to intermediate values, such as 0.50 pu. The region of these nodes is highlighted in blue in Figure 6.

Load power As showed before, in the 13 and 34 nodes system, the highest loads are respectively in nodes 671-675 and 890-844, highlighted in red in Figure 5 and 6. Where the optimized PP are the minimum limits for the active power, but for the reactive occurred the opposite, the parameter go to maximum when reactive injection was allowed. This situation results from an injection of active power, whose nominal values are higher than the reactive, raise the mains voltage and consequently the fault current, even at the lower limit. Thus to compensate for the impact of this high volume of power, the system injects maximum limit of reactive, since the smaller ones could not compensate for this increase.

Location In the analysis with and without reactive injection permission, the expected values were minimal in both situations, but the opposite occurred in the central branch region of the 34 nodes system, between node 824 to 832, highlighted in green in Figure 6. Instead of going from zero to -0.44, optimization converged to keep PP at zero. This result comes from the fact that a reactive injection, keeping the active power constant, would result in an increase of the voltage and the fault current, hence the previous decision to keep the setting value at zero.

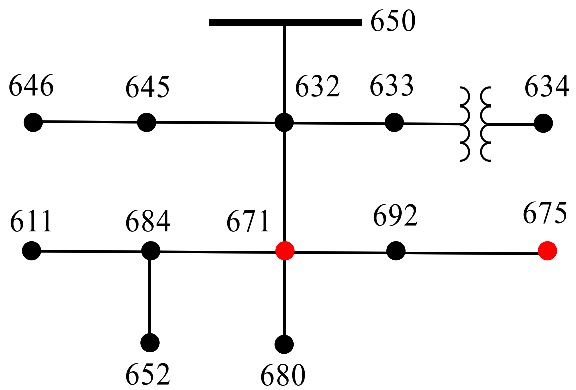

Figure 5. IEEE Test Feeder 13 nodes, category Zero and B.

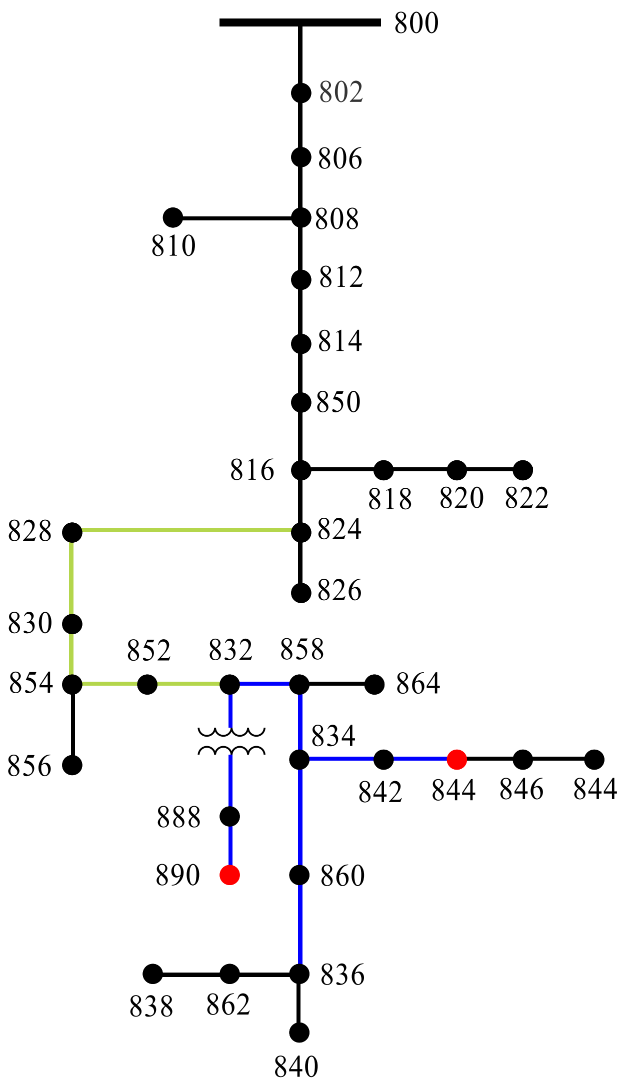

Figure 6. IEEE Test Feeder 34 nodes, category Zero and B.

4. CONCLUSION

The use of optimization to obtain the power parameters for DG was satisfactory, considering the convergence of the system to values within the established constraints. The choice of minimizing the single phase and three phase fault current met the proposal of obtaining parameters that guarantee greater protection to the nodes in a scenario of high penetration of distributed generation. The lower OF value occurring in category B was an expected result since the variables have a longer interval to search for the local optimum values. As well as the worst minimization occurs in category Zero, where there is no reactive power injection, since the range is the smallest. The difference between the two categories is 0.636% for 13-node and 0.818% for 34-node. Another factor that influenced the process of PP optimization was the input parameters, which are particular to each system. In nodes whose load power parameter was higher the variables values was the minimum limits for the active and the maximum for the reactive power. From the results, it is noted that not only the load value, and consequently of the DG, influences the short circuit current, but also its location and neighborhood, reinforcing the need for further studies in scenarios with an increasing number of elements.

REFERENCES

Baghaee, H.R., Kaviani, A.K., Mirsalim, M., and Ghareh-petian, G.B. (2011). Short circuit level and loss reduction by allocating tcsc and upfc using particle swarm optimization. In *2011 19th Iranian Conference on Electrical Engineering*, 1–1.

Chang, G.W., Chu, S.Y., and Wang, H.L. (2007). An improved backward/forward sweep load flow algorithm for radial distribution systems. *IEEE Transactions on Power Systems*, 22(2), 882–884. doi:10.1109/TPWRS.2007.894848.

Cui-Ru Wang, He-Jin Yuan, Zhi-Qiang Huang, Jiang-Wei Zhang, and Chen-Jun Sun (2005). A modified particle swarm optimization algorithm and its application in optimal power flow problem. In *2005 International Conference on Machine Learning and Cybernetics*, volume 5, 2885–2889 Vol. 5. doi:10.1109/ICMLC.2005.1527435.

d. S. Barbosa, A. and Carvalho, P.L. (2017). Impacts of the change in regulation in brazil: penalty simulation for violation of collective interruption indicators versus compensation for consumers. *CIRED - Open Access Proceedings Journal*, 2017(1), 729–732. doi:10.1049/oap-cired.2017.0676.

Ferraz, R.S.F., Ferraz, R.S.F., de Lima, R.C.D., Tonini, L.G.R., Rueda-Medina, A.C., and Batista, O.E. (2019). Genetic optimization-based overcurrent relay coordination in a feeder with high distributed generation integration. In *2019 IEEE PES Innovative Smart Grid Technologies Conference - Latin America (ISGT Latin America)*, 1–6. doi:10.1109/ISGT-LA.2019.8894961.

IEEE (2018). Ieee draft standard conformance test procedures for equipment interconnecting distributed energy resources with electric power systems and associated interfaces. *IEEE P1547.1/D9.7, February 2018*, 1–283.

Jangra, J. and Vadhera, S. (2017). Load flow analysis for three phase unbalanced distribution feeders using matlab. In *2017 2nd International Conference for Convergence in Technology (I2CT)*, 862–866. doi:10.1109/I2CT.2017.8226252.

Kennedy, J. and Eberhart, R. (1995). Particle swarm optimization. In *Proceedings of ICNN'95 - International Conference on Neural Networks*, volume 4, 1942–1948 vol.4. doi:10.1109/ICNN.1995.488968.

Kersting, W.H. and Shirek, G. (2012). Short circuit analysis of ieee test feeders. In *PES T D 2012*, 1–9. doi:10.1109/TDC.2012.6281539.

Mendes, M.A., Vargas, M.C., Batista, O.E., and Simonetti, D.S.L. (2018). A review on the methods for mitigate the impacts of photovoltaic distributed generation in power systems protection. In *2018 Simposio Brasileiro de Sistemas Eletricos (SBSE)*, 1–6. doi:10.1109/SBSE.2018.8395867.

Rueda-Medina, A.C. and Padilha-Feltrin, A. (2011). Optimal allocation of distributed generators providing reactive power support ancillary service. In *2011 IEEE Trondheim PowerTech*, 1–6. doi:10.1109/PTC.2011.6019165.

Tonini, L.G.R., Batista, O.E., Rueda-Medina, A.C., Mendes, M.A., and Vargas, M.C (2019). Power flow analysis on networks with high integration of distributed photovoltaic generation. In *2019 IEEE PES Innovative Smart Grid Technologies Conference - Latin America (ISGT Latin America)*, 1–6. doi:10.1109/ISGT-LA.2019.8895415.

Vargas, M.C., Mendes, M.A., Batista, O.E., and Simonetti, D.S.L. (2018). A review on the protection elements required for distributed generation in brazil. In *2018 Simposio Brasileiro de Sistemas Eletricos (SBSE)*, 1–6. doi:10.1109/SBSE.2018.8395905.

Appendix A. OPTIMIZED PP

Table A.1. Category Zero, A and B, for IEEE Test Feeder 34 nodes

Node	Fase	P_{Zero}	P_A	P_B	Q_{Zero}	Q_A	Q_B
802	B	1.00	1.00	1.00	0.00	-0.22	-0.44
	C	0.05	0.05	0.05	0.44	0.44	0.44
806	B	0.50	0.50	0.50	0.44	0.22	0.00
	C	0.05	0.05	0.05	0.00	-0.22	-0.44
808	B	0.50	0.50	0.50	0.00	0.00	-0.44
810	B	0.50	0.05	0.05	0.44	0.22	0.44
816	B	1.00	1.00	1.00	0.00	0.00	0.00
818	A	1.00	1.00	1.00	0.44	0.22	0.44
820	A	0.50	0.50	0.50	0.00	-0.22	-0.44
822	A	1.00	1.00	1.00	0.44	0.44	0.44
824	B	0.05	0.05	0.05	0.00	0.00	-0.44
	C	1.00	1.00	1.00	0.00	0.00	0.00
826	B	0.50	0.50	0.50	0.44	0.44	0.44
828	A	0.05	0.05	0.05	0.00	0.00	0.00
	C	0.50	0.50	0.50	0.00	0.00	0.00
830	A	1.00	1.00	1.00	0.00	0.00	0.00
854	B	0.50	0.50	0.50	0.00	0.00	0.00
856	B	1.00	1.00	1.00	0.00	0.00	0.00
832	A	0.50	0.50	0.05	0.44	0.44	0.44
	B	1.00	1.00	1.00	0.00	0.00	0.00
	C	1.00	1.00	1.00	0.00	0.00	0.00
858	A	1.00	1.00	1.00	0.00	0.00	-0.44
	B	0.50	0.50	0.05	0.44	0.22	0.44
	C	0.50	0.50	0.50	0.44	0.00	0.00
864	A	1.00	1.00	1.00	0.00	0.00	0.00
834	A	0.50	0.50	0.50	0.00	-0.22	-0.44
	B	0.05	0.50	0.05	0.44	0.44	0.44
	C	0.05	0.50	0.05	0.44	0.44	0.44
842	A	0.50	0.50	0.05	0.00	0.22	0.00
846	B	0.05	0.50	0.05	0.44	0.44	0.44
	C	1.00	1.00	1.00	0.00	-0.22	-0.44
836	A	0.50	0.50	0.50	0.00	-0.22	-0.44
	B	0.50	0.50	0.05	0.00	-0.22	-0.44
	C	0.50	0.50	0.05	0.44	0.22	0.00
862	B	0.50	0.50	0.50	0.44	0.22	0.44
838	B	0.50	0.50	0.50	0.00	0.00	-0.44
860	A	1.00	1.00	1.00	0.00	0.00	-0.44
	B	0.50	0.50	0.50	0.44	0.22	0.44
	C	1.00	1.00	1.00	0.00	-0.22	-0.44
840	A	1.00	1.00	1.00	0.44	0.00	-0.44
	B	0.50	0.50	0.50	0.44	0.22	0.44
844	A	0.05	0.05	0.05	0.00	-0.22	-0.44
	B	0.05	0.05	0.05	0.44	0.44	0.44
	C	0.50	0.50	0.50	0.44	0.44	0.44
848	A	1.00	1.00	1.00	0.00	0.22	0.00
	B	1.00	1.00	1.00	0.00	0.00	-0.44
	C	0.05	0.50	0.05	0.00	0.00	-0.44
890	A	0.50	0.50	1.00	0.00	0.00	-0.44
	B	0.50	0.50	0.50	0.44	0.22	0.00
	C	0.05	0.05	0.05	0.44	0.22	0.00

Table A.2. Category Zero, A and B, for IEEE Test Feeder 13 nodes

Node	Fase	P_{Zero}	P_A	P_B	Q_{Zero}	Q_A	Q_B
632	A	0.05	0.05	0.05	0.00	0.00	-0.44
	B	0.05	1.00	0.05	0.00	0.44	-0.44
	C	1.00	0.05	1.00	0.44	-0.22	0.44
634	A	0.05	1.00	1.00	0.00	0.44	-0.44
	B	1.00	1.00	0.05	0.44	-0.22	0.44
	C	1.00	0.05	1.00	0.44	0.44	0.44
645	B	0.05	0.05	0.05	0.44	-0.22	0.44
646	B	0.05	0.05	0.05	0.44	0.44	0.44
671	A	0.05	1.00	0.05	0.00	0.44	-0.44
	B	0.05	0.05	0.05	0.00	-0.22	0.44
	C	1.00	0.05	1.00	0.44	0.44	0.44
692	C	1.00	0.05	1.00	0.44	0.44	-0.44
675	A	0.05	1.00	0.05	0.00	0.44	0.44
	B	0.05	0.05	0.05	0.00	0.44	0.44
	C	1.00	0.05	1.00	0.44	0.44	0.44
652	A	1.00	1.00	1.00	0.00	0.44	-0.44
611	C	1.00	0.05	1.00	0.44	0.44	0.44